

Corrosion of Reinforcing Bars Embedded in Alkali-activated Slag Concrete Subjected to Chloride Attack

William Aperador Chaparro^{a*}, Jorge Hernando Bautista Ruiz^b,

Robinson De Jesús Torres Gómez^c

^aDepartment of Mechatronics Engineering, Universidad Militar Nueva Granada, Bogotá D.C., Colombia

^bBasic Science Faculty, Universidad Francisco de Paula Santander, A.A 12215, San José de Cúcuta, Colombia

^cDepartment of Metallurgical Engineering, Universidad Pedagógica y Tecnológica de Colombia, Autopista Norte, Tunja, Colombia

Received: May 23, 2011; Revised: November 9, 2011

Steel bar embedded in an alkali-activated slag (AAS) concrete was tested under complete immersion, in 3.5% NaCl solution by weight of the slag. Ordinary Portland cement (OPC) was also tested for comparative purposes and exposed to the same solution. Monitoring of open-circuit potential, polarization resistance measurement and electrochemical impedance spectroscopy (EIS) were used to evaluate the corrosion behavior of steel bar. The corrosion resistances of AAS and OPC concretes were performed at 0, 3, 6, 9 and 12 months. Electrochemical measurements shows that AAS concrete presents passive corrosion behavior the first 3 months, after this period of time, it presents corrosion resistance decreased due to the chlorides presence at the steel/AAS interface. For 0 months immersion (28 days of curing) the AAS and OPC concretes presented a 10% of corrosion probability. After 3 months of immersion the tested AAS and OPC concretes showed similar behavior, the active potentials in the range from -0.2 to -0.6 V vs. Cu/CuSO₄ indicate a 90% probability of corrosion.

Keywords: corrosion, alkali-activated cement, chloride ion, electrochemical measurements

1. Introduction

The nature and integrity of solid layer hydration products formed in close proximity to the embedded steel can be an important role in metal controlling passivation and depassivation.

In spite of the advantages of reinforced concrete, corrosion of the steel bar remains its most common durability problem¹. The most important cause of corrosion initiation of steel bar is the ingress of chloride ions to the steel surface²⁻⁴. Corrosion of steel bar damages the reinforced concrete structures in two ways: First, it reduces the cross-sectional area of steel bar. Second, it produces corrosion products with a larger volume than the steel itself. The volume increase induces the tensile stress in concrete, which results in cracking and eventual structural failure^{5,6}.

Granulated blast-furnace slag (GBFS) has been used for many years as a supplementary cementitious material in ordinary Portland cement (OPC) concrete, either as a mineral admixture or as a component of blended cement. Doubts have been raised about the use of GBFS in pre-stressed and post-tensioned concrete. GBFSs contain sulphides that can catalyze the development of hydrogen atoms when pre-stressed steel embedded in concrete corrodes, thus leading to hydrogen embrittlement. Nevertheless, tests and practical experience over 50 years have shown that such concern is not justified and GBFS cement can be freely used^{7,8}.

In an attempt to overcome these problems, the construction sector is very interested in the development of new cement binder materials as an alternative to OPC^{9,10}. In this respect, the most promising emerging approach is based on raw materials suitable for alkaline activation, which originate new binding materials generically known as alkaline cements^{11,12}. The use of slag as supplementary cementitious material improves the durability of concrete as it reduces the chloride penetration achieved by GBFS has been confirmed by many different investigators^{13,14}.

The aim of this paper is to study the corrosion properties of steel rebars embedded in alkaline active slag and exposed 3.5% NaCl solution by weight of the slag. For comparative purposes, steel rebars were embedded in OPC in identical experimental conditions. The specimens were studied using corrosion potential, linear polarization resistance, and electrochemical impedance spectroscopy methods.

2. Experimental

GBFS from the company "Acerías Paz del Río", located at Boyacá, Colombia, was used with a chemical composition (% by weight) of 33.7 SiO₂, 12.8 Al₂O₃, 3.09 Fe₂O₃, 45.4 CaO, 0.5 TiO₂, 0.64 SO₃, 1.79 MgO and 2.08 loss ignition, a specific surface area of 398 m².kg⁻¹ and a specific gravity of 2860 kg.m⁻³. The basicity (CaO + MgO / SiO₂

*e-mail: g.ing.materiales@gmail.com

+ Al₂O₃) and quality (CaO + MgO + Al₂O₃ / SiO₂ + TiO₂) indexes were 1.01 and 1.73, respectively. According to ASTM C 989-99 Standard this material was grade 80 slag¹⁵. The waterglass used as the activating solution consisted of a commercial sodium silicate mix (31.7% SiO₂, 12.3% Na₂O and 56.0% water) with a 50% NaOH solution to obtain a SiO₂/Na₂O ratio of 2.4. The Na₂O concentration in the waterglass activating solution added to the concrete was 5% by weight of slag. The aggregate used was a siliceous gravel with a maximum grain size of 19 mm, specific gravity of 2940 kg.m⁻³, and 1.3% absorption, and river sand with a maximum grain size of 19 mm, a specific gravity of 2470 kg.m³, and 2.9% absorption. OPC according to ASTM C 150-02 Standard was used for comparative purposes¹⁶⁻¹⁸, with a specific gravity and specific surface area of 2990 and 400 kg.m⁻³, respectively. AAS and OPC concretes were prepared with a water/cement ratio of 0.4.

The AAS and OPC specimens were cured in a climatic chamber for 28 days at 90% relative humidity (RH) for AAS specimens and at 100% RH for OPC specimens to prevent leaching of the activating solutions and to assure that the hydration reaction and product formation processes were not affected.

Structural 1018 steel bars of 6.35 mm diameter were used, according to ASTM A 706-08 Standard¹⁷. A cylindrical reinforced concrete specimen (76.2 mm diameter and 76.2 mm length) was used to perform the experimental tests.

Electrochemical measurements were carried out by immersing the specimens completely in 3.5% NaCl solution by weight of the slag with a classic 3-electrode configuration, using the steel bars as working electrode, a graphite bar as counter electrode, and a copper/copper sulphate (Cu/CuSO₄) reference electrode. An active surface area of 10 cm² was marked on the working electrode with an epoxy resin, thus isolating the triple concrete/steel/atmosphere interface to avoid a possible localized corrosion attack due to differential aeration. Finally, for analyzed corrosion surface process, the superficial morphology was characterized by using a High-Resolution Scanning Electron Microscope (SEM) (Philips® XL 30 FEG).

Steel bar corrosion over time was monitored by using three techniques: (i) Corrosion potential (E_{corr}) values. The E_{corr} parameter may be used to define the probability for OPC/carbon steel system: for $E_{\text{corr}} < -0.35$ V vs. Cu/CuSO₄ high corrosion probability (~90%), for $-0.35 < E_{\text{corr}} < -0.20$ V vs. Cu/CuSO₄ uncertainty of corrosion, and for $E_{\text{corr}} > -0.20$ V vs. Cu/CuSO₄ a 10% probability of corrosion¹⁶; (ii) Linear polarization resistance (R_p) values.

$$R_p = \frac{\Delta E}{\Delta I} \quad (1)$$

The steel corrosion rate can be calculated from the Stern-Geary Equation¹⁹:

$$i_{\text{corr}} = \frac{B}{R_p} \quad (2)$$

applying $\Delta E \pm 20$ mV at a scan rate of 0.16 mV/s, A tentative value of 52 or 26 mV for the B constant for steel in the passive or active (corroding) state, respectively. The corrosion level

for OPC/carbon steel system may be defined according to the Durar Network Specification¹⁶: for $i_{\text{corr}} < 0.1$ $\mu\text{A}\cdot\text{cm}^{-2}$ passivity, for $0.1 \mu\text{A}\cdot\text{cm}^{-2} < i_{\text{corr}} < 0.5 \mu\text{A}\cdot\text{cm}^{-2}$ low corrosion, for $0.5 \mu\text{A}\cdot\text{cm}^{-2} < i_{\text{corr}} < 1.0 \mu\text{A}\cdot\text{cm}^{-2}$ high corrosion, and for $i_{\text{corr}} > 1.0 \mu\text{A}\cdot\text{cm}^{-2}$ very high corrosion; and (iii) Electrochemical impedance spectroscopy (EIS). EIS measurements were recorded at the E_{corr} in a frequency range from 1×10^5 to 1×10^{-3} Hz with a logarithmic sweeping frequency of 3 points per decade. The EIS method involved the imposition of a 10 mV amplitude excitation voltage. A Gamry model PCI 4 workstation was utilized for DC and AC measurements. Electrochemical measurements were performed at 0, 3, 6, 9 and 12 months for AAS and OPC specimens.

3. Results and Discussion

Figure 1 shows the evolution of the rebar corrosion potential (E_{corr}) measured on AAS and OPC concrete exposed to 3.5% NaCl solution by weight of the slag, during 12 months immersion. For 0 months immersion (28 days of curing) the AAS and OPC concretes presented a 10% probability of corrosion, corresponding to a state of passivity based on the Pourbaix diagram. After 3 months of immersion the tested AAS and OPC concretes showed similar behavior, the active potentials in the range from -0.2 to -0.6 V vs. Cu/CuSO₄ indicate presented a 10% of corrosion probability. E_{corr} evolutions of OPC concrete were constant after 6 months, AAS specimen present the most negative corrosion potential values after 6 months.

Figure 2 shows R_p and i_{corr} values vs. time for steel rebar embedded in AAS and OPC concrete. The AAS and OPC specimens showed the highest R_p values for 0 months immersion. The R_p values decrease showed the lowest R_p values after 3 months; with R_p values in the range from

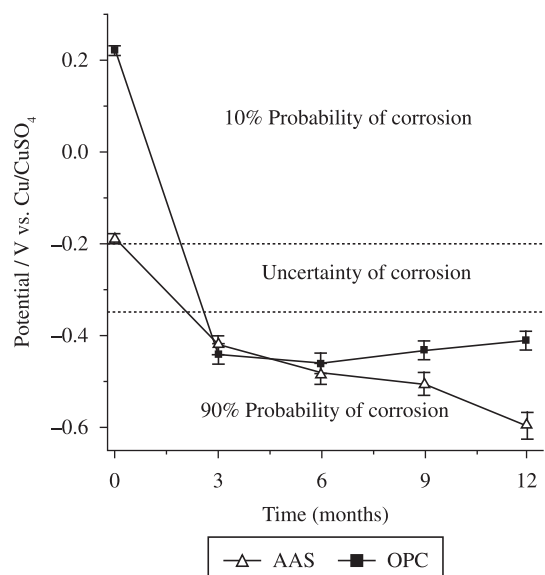


Figure 1. Corrosion potential (E_{corr}) vs. time for steel rebars embedded in AAS and OPC concretes, immersed in a 3.5% NaCl solution by weight of the slag.

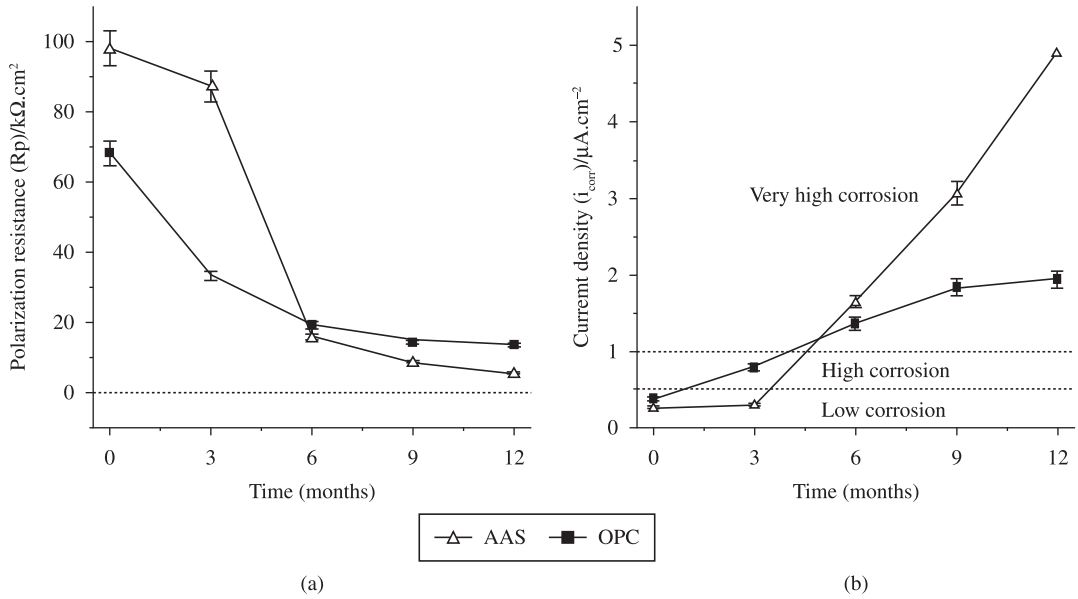


Figure 2. Polarization resistance (R_p) and current density (i_{corr}) vs. time for steel rebars embedded in AAS and OPC concretes immersed in a 3.5% NaCl solution by weight of the slag.

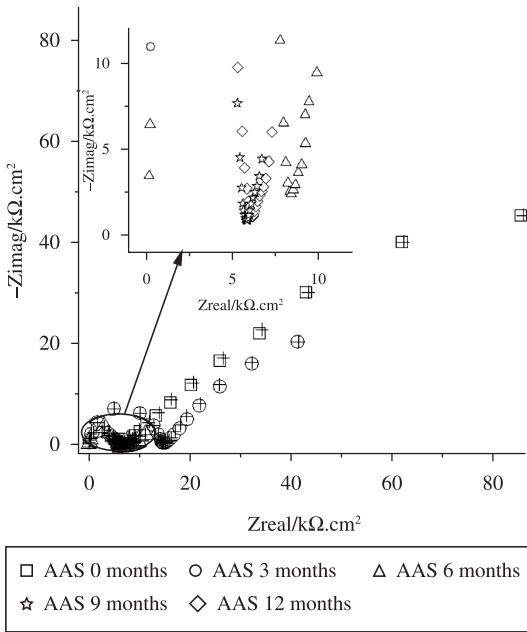


Figure 3. Nyquist plots for steel rebars embedded in AAS concrete exposed to 3.5% NaCl solution by weight of the slag.

87 to 5 $k\Omega \cdot cm^2$ for AAS and 33 to 13 $k\Omega \cdot cm^2$ (Figure 2a). Figure 2b presents corrosion current density (i_{corr}) values, estimated from the R_p measurements using the Stern-Geary equation¹⁹, vs. time for steel rebar embedded in the two concretes. The AAS and OPC concrete after 0 months, present similar i_{corr} showed lower corrosion current densities of 0.2 and 0.3 $\mu A \cdot cm^{-2}$, respectively (Figure 2b). According to the classification proposed by Durar Network Specification,

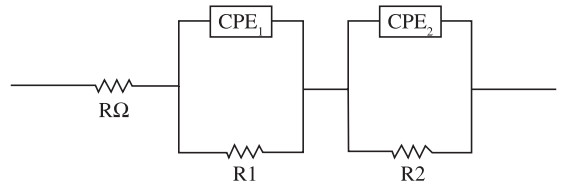


Figure 4. Electrical equivalent circuit used to fit impedance data of steel embedded in AAS and OPC concretes. R_Ω is the electrolyte/concrete interface resistance; CPE_1 and CPE_2 are constant phase elements defined at high and low frequency, respectively; R_1 is the pore solution resistance; and R_2 is the charge transfer resistance (corrosion).

this value means generally low corrosion¹⁶. The behavior of AAS specimen varied in time, i_{corr} presents an increased trend during the first 3 months, after this period of time the rebar corrosion current density increased values assumed as the threshold between low corrosion and very high corrosion for 12 months. The OPC concrete showed the highest i_{corr} , with a value of 0.8 $\mu A \cdot cm^{-2}$ (high corrosion) after 3 months and 2 $\mu A \cdot cm^{-2}$ (very high corrosion) after 12 months.

Figure 3 shows typical Nyquist plots for steel rebar embedded in AAS concrete exposed to 3.5% NaCl solution by weight of the slag. Measurements were performed at 0 (28 days of curing), 3, 6, 9 and 12 months. Table 1 includes fitting data yielded using the equivalent circuit of Figure 4. In general, a capacitive behavior was obtained, characterized by a poorly defined and depressed semicircle at high frequencies and a second semicircle associated to the steel corrosion process at low frequencies.

Figure 5 shows typical Nyquist plots for steel rebar embedded in OPC concrete, exposed to same conditions AAS specimens. Table 1 includes fitting data yielded using

Table 1. Parameters used in the fitting of impedance data for steel rebars embedded in alkali-activated slag (AAS) and OPC concretes immersed in a 3.5 wt. (%) NaCl solution.

Time (months)	R_{Ω} ($\Omega \cdot \text{cm}^2$)	Y_{p1} ($F\text{cm}^{-2} s^{-(1-\alpha_1)}$)	α_1	R_1 ($\text{k}\Omega \cdot \text{cm}^2$)	Y_{p2} ($F\text{cm}^{-2} s^{-(1-\alpha_2)}$)	α_2	R_2 ($\text{k}\Omega \cdot \text{cm}^2$)
AAS concrete							
0	602.0	0.12×10^{-8}	0.59	13.4	1.83×10^{-3}	0.52	85.13
3	68.0	0.45×10^{-8}	0.75	3.67	104×10^{-3}	0.85	12.6
6	53.2	0.64×10^{-8}	0.87	2.45	171×10^{-3}	0.93	11.3
9	40.6	0.93×10^{-8}	0.93	1.72	221×10^{-3}	0.86	7.19
12	27.3	2.71×10^{-8}	0.86	0.57	234×10^{-3}	0.72	6.75
OPC concrete							
0	645.3	0.010×10^{-8}	0.81	15.9	2.74×10^{-3}	0.86	58.0
3	36.7	0.140×10^{-8}	0.87	1.13	11.9×10^{-3}	0.75	14.4
6	42.7	0.199×10^{-8}	0.79	0.80	15.8×10^{-3}	0.78	11.4
9	34.1	0.24×10^{-8}	0.84	0.73	17.6×10^{-3}	0.83	10.3
12	29.1	0.276×10^{-8}	0.92	0.59	25.7×10^{-3}	0.92	7.4

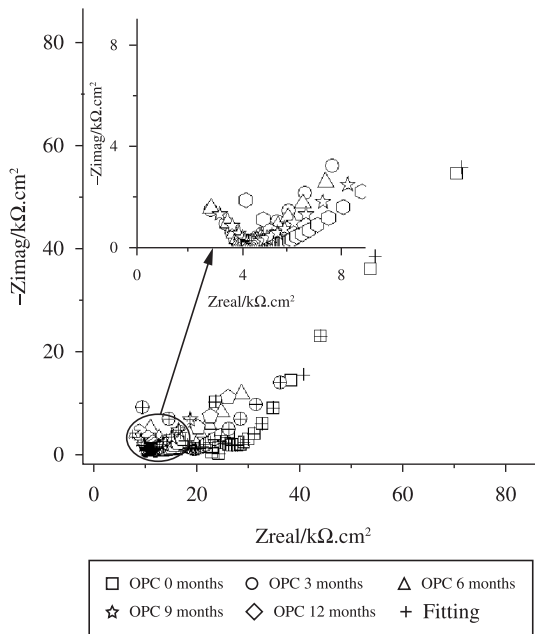


Figure 5. Nyquist plots after 108 days of experimentation for steel rebars embedded in OPC concrete exposed to 3.5 wt. (%) NaCl solution at 25 °C.

the equivalent circuit of Figure 4. In general, as for OPC concrete, a capacitive behavior was observed, characterized by a poorly defined semicircle at high frequencies and a second semicircle at low frequencies.

Equivalent circuit of Figure 4 contains two distributed constant phase elements (CPE_1 and CPE_2) to consider the two relaxation time constants (Figures 3 and 5). The CPE_1-R_1 couple, which predominates at high frequencies, may be originated by the passive film and/or the dielectric properties of the concrete, while the CPE_2-R_2 couple, controlled at low frequencies, characterizes the corrosion process of the steel/concrete pore solution interface. R_{Ω} is the electrolyte resistance.

Distributed CPEs are widely used in data fitting to allow for depressed semicircles. The depressed semicircle is generally due to a dispersion in the time constant, caused by irregularities on the steel surface, surface roughness, fractal surface, and in general certain processes associated with an irregular distribution of the applied potential (10 mV) to obtain EIS data. The admittance representation of a CPE (Y_{CPE}) shows a fractional-power dependent on the angular frequency (ω):

$$Y_{CPE} = Y_p(j\omega)^{\alpha} \quad (3)$$

where Y_p is a real adjustable constant used in the non-linear least squares (NLLS) fitting, and $-1 < \alpha < 1$ defined as a CPE power.

Table 1 includes optimized fitting impedance parameter values for the AAS/steel and OPC/steel system. The high frequency process had a CPE_1 (Y_{p1}) for AAS in the range from 0.12×10^{-8} to $2.71 \times 10^{-8} F\text{cm}^{-2} s^{-(1-\alpha_1)}$, for OPC in the range from 0.1×10^{-9} to $2.76 \times 10^{-9} F\text{cm}^{-2} s^{-(1-\alpha_1)}$. The optimized values for the various parameters are given in Table 1. At lower frequencies a capacitive behavior was observed indicating a situation of passivity for AAS and OPC after 0 months, these value capacitive increments indicating the active condition of the rebar after 3 months of exposure OPC concrete and 6 months for AAS specimens.

Although the R_2 (corrosion resistance) values for the AAS/steel and OPC/steel system decreased with time, showed a low corrosion resistance after 3 months, see R_2 values in Table 1.

The impedance data could be interpreted in the following way. During the first 3 months of testing, the steel appears to show certain inertia to starting the corrosion process due to the passivation of the steel. The fitting process gives a R_2 value from 86 to 7 $\text{k}\Omega \cdot \text{cm}^2$ for AAS concrete (Table 1). The effect of chloride content in AAS concrete show that R_2 decreases when the time of exposition increases. Accepting that the Stern-Geary equation can be applied, with an approximate B constant value of 26 mV, the resulting corrosion current density is low ($i_{\text{corr}} = 0.3 \mu\text{A} \cdot \text{cm}^{-2}$),

which is not far from the i_{corr} results obtained using the R_p measurements (Figure 2b).

For the OPC/steel system the EIS results show a similar picture, with a depressed semicircle at high frequencies and a second semicircle also depressed at low frequencies, yielding an R_2 value from 58 to 7 $\text{k}\Omega\cdot\text{cm}^2$ (Table 1). The estimated corrosion current density was low, of the order of $0.4 \mu\text{A}\cdot\text{cm}^{-2}$. These results agree well with the DC data, see Figure 2b.

A way to determine the kind of corrosion of the materials consist in analyze the morphology of the products generated in the process (oxides and hydroxides). This analysis complements the information obtained by means of field or laboratory electrochemical techniques.

The embedded steel in OPC concrete, in aggressive conditions presented a homogenous distribution of the corrosion products (Figure 6). However when observing bigger increases, it can be noticeable how this cape of oxides do not appear in the totality metal surface. This agrees with the electrochemical data obtained, because although stable values of polarization resistance regarding time are showed, they were not high enough due to the formation of oxide capes not much uniforms.

In aggressive environments, where the chloride was exposed to steel to the chloride ions, it is impossible to evidence the formation of protective films above the same (Figure 7). A uniform protective oxides cape on metal was not generated and the distribution was not homogenous. On the contrary small groups take shape and appear like elements with a darker tonality. Besides it can become evident than ions chloride they break the oxide cape producing a porous surface that does not protect the steel. This is the reason why the polarization resistance in these materials present low values.

The conditions of passivity found in AAS concrete in conditions without treatment are explained by means of SEM observations. It was observed a homogeneous film on metal (Figure 8). This included a group of outstands oxides at some places like small shapely groups on the surface.

Nevertheless, when this film with good protective properties is attacked by the chloride ions loses great part of its characteristics. The steel of the AAS concrete does not lose the passive film completely (Figure 9). Next of

the exposition in aggressive environments exist still small oxide crowds on the surface of steel. The inconvenience that these corrosion products consists in that its structure is dense but suffer of cracking that they allow the pass of other contaminants.

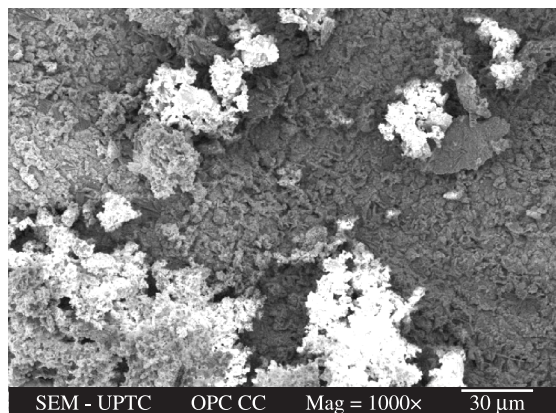


Figure 7. Surface of the steel embedded in OPC concrete exposed to 3.5 wt. (%) NaCl solution at 25 °C.

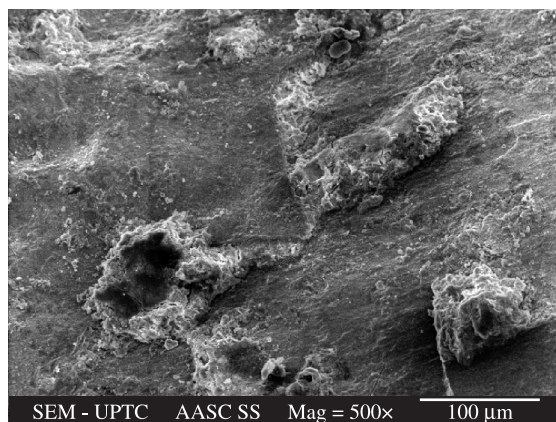


Figure 8. Surface of the steel embedded in AAS concrete, without treatment.

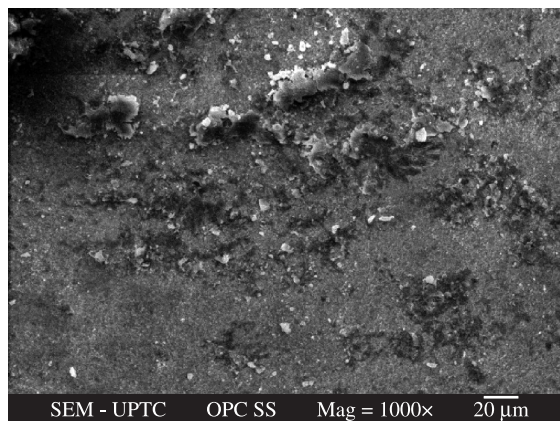


Figure 6. Surface of the steel embedded in OPC concrete, without treatment.

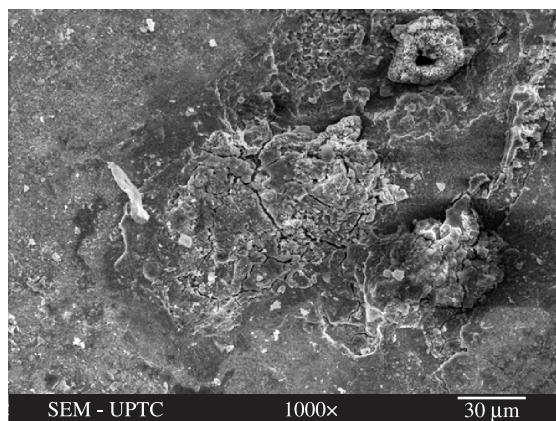


Figure 9. Surface of the steel embedded in AAS concrete exposed to 3.5% NaCl solution by weight of the slag.

4. Conclusions

The open circuit potential values of the AAS concrete samples immersed in a saline solution for 3 months allows predicting the starting time of the corrosive process in the AAS reinforced concrete structures.

The electrochemical impedance spectroscopy is a powerful technique for analyzing the behavior of the electrical characteristics of AAS concrete generated by the migration of chloride ions. The chloride ions in the concrete decrease the polarization resistance values. At low frequencies, the capacitance value increases due to the concrete-steel interface. These results correlate with the reported values of R_p .

For 0 months immersion (28 days of curing) the AAS and OPC concretes presented a 10% probability of corrosion. After 3 months of immersion the tested AAS and OPC concretes showed similar behavior, the active potentials in the range from -0.2 to -0.6 V vs. Cu/CuSO_4 indicate a 90% probability of corrosion

Acknowledgements

W. Aperador expresses his gratitude to the Centre of Excellence in Novel Materials (CENM) and COLCIENCIAS of Colombia, Project Geoconcret, for the scholarship granted to him.

References

- Chung L, Jay JH and Yi ST. Bond strength prediction for reinforced concrete members with highly corroded reinforcing bars. *Cement and Concrete Composites*. 2008; 30(7):603-611. <http://dx.doi.org/10.1016/j.cemconcomp.2008.03.006>
- Meira GR, Andrade C, Padaratz IJ, Alonso C and Borba Junior JC. Chloride penetration into concrete structures in the marine atmosphere zone - relationship between deposition of chlorides on the wet candle and chlorides accumulated into concrete. *Cement and Concrete Composites*. 2007; 29 (9):667-676. <http://dx.doi.org/10.1016/j.cemconcomp.2007.05.009>
- Bastidas DM, Fernández-Jiménez A, Palomo A and González JA. A study on the passive state stability of steel embedded in activated fly ash mortars. *Corrosion Science*. 2008;50(4):1058-1065. <http://dx.doi.org/10.1016/j.corsci.2007.11.016>
- Arya C and Xu Y. Effect of cement type on chloride binding and corrosion of steel in concrete. *Cement and Concrete Research*. 1995; 25(4):893-902. [http://dx.doi.org/10.1016/0008-8846\(95\)00080-V](http://dx.doi.org/10.1016/0008-8846(95)00080-V)
- Choi YS, Kim JG and Lee KM. Corrosion behavior of steel bar embedded in fly ash concrete. *Corrosion Science*. 2006; 48(7):1733-1745. <http://dx.doi.org/10.1016/j.corsci.2005.05.019>
- Song HW and Saraswathy V. Studies on the corrosion resistance of reinforced steel in concrete with ground granulated blast-furnace slag. An overview. *Journal of Hazardous Materials*. 2006;138 (2):226-233. <http://dx.doi.org/10.1016/j.jhazmat.2006.07.022>
- Aperador W, Mejía de Gutiérrez R and Bastidas DM. Steel corrosion behaviour in carbonated alkali-activated slag concrete. *Corrosion Science*. 2009; 51(9):2027-2033. <http://dx.doi.org/10.1016/j.corsci.2009.05.033>
- Torres R, Aperador W, Vera E, Ortiz C and Mejía de Gutierrez R. Estudio de la corrosión del acero embebido en Concreto aas sometido a cloruros. *Dyna*. 2010; 77(164):52-59
- Fernández-Jimenez A and Puertas F. Effect of activator mix on the hydration and strength behavior of alkali-activated slag cements. *Advances in Cement Research*. 2003;15(3):129-136. <http://dx.doi.org/10.1680/adcr.2003.15.3.129>
- Fernández-Jiménez A, Miranda JM, González JA and Palomo A. Steel passive state stability in activated fly ash mortars. *Materiales de Construcción*. 2010; 60(300):51-65
- Elakneswaran Y, Nawa T and Kurumisawa K. Zeta potential study of paste blends with slag. *Cem. Concr. Comp.* 2009;31(1):72-76. <http://dx.doi.org/10.1016/j.cemconcomp.2008.09.007>
- Ahmed MS, Kayali O and Anderson W. Chloride penetration in binary and ternary blended cement concretes as measured by two different rapid methods. *Cement and Concrete Composites*. 2008; 30 (7):576-582. <http://dx.doi.org/10.1016/j.cemconcomp.2008.02.005>
- Puertas F, Gil-Maroto A, Palacios M and Amat T. Alkali-activated slag mortars reinforced with a glass fibre. Performance and properties. *Materiales de Construcción*. 2006; 56 (283):79-90.
- Roy DM, Jiang W and Silsbee MR. Chloride diffusion in ordinary, blended, and alkali-activated cement pastes and its relation to other properties. *Cement and Concrete Research*. 2000; 30(12):1879-1884. [http://dx.doi.org/10.1016/S0008-8846\(00\)00406-3](http://dx.doi.org/10.1016/S0008-8846(00)00406-3)
- American Society for Testing and Materials - ASTM. *ASTM C 989-99 Standard*: Standard specification for ground granulated blast-furnace slag for use in concrete and mortars. West Conshohocken: American Society for Testing and Materials, 1999.
- American Society for Testing and Materials - ASTM. *ASTM C 150-02 Standard*: Specification for Portland cement test. West Conshohocken: American Society for Testing and Materials, 2002.
- American Society for Testing and Materials - ASTM. *ASTMA 706-08 Standard*: Standard specification for low-alloy steel deformed and plain bars for concrete reinforcement. West Conshohocken: American Society for Testing and Materials, 2008.
- Durar Network. Manual de Inspección, Evaluación y Diagnóstico de Corrosión en Estructuras de Hormigón Armado. CYTED Programe, 1997.
- Stern M and Geary AL. Electrochemical polarization I. A theoretical analysis of the shape of polarization curves. *Journal of the Electrochemical Society*. 1957;104 (1):56-63. <http://dx.doi.org/10.1149/1.2428496>